Effect of shoulder angle variation on sEMG-based elbow joint angle estimation

Zhichuan Tang*, Hongchun Yang, Lekai Zhang, Pengcheng Liu

Abstract

For the decade now, surface electromyogram (sEMG) signal has been extensively applied in joint angle estimation to control the prostheses and exoskeleton systems. However, the sEMG signal patterns can be severely affected by shoulder angle variations, which restricts its applications to a practical use. In our study, we evaluate the effect of shoulder angle variations on elbow angle estimation performance. This adverse effect increases mean root mean square (RMS) error by $14.85°$ in our experiment. Then, four estimation methods are proposed to solve this problem: (1) using a training set including all shoulder angles' training data to train model; (2) adding two shoulder muscles' sEMG as additional inputs; (3) a two-step method using arm muscles' sEMG and two shoulder muscles' sEMG; and (4) a two-step method using arm muscles' sEMG and measured shoulder angle value by a motion sensor. 13 subjects are employed in this study. The experimental results demonstrate that the mean RMS error is reduced from $21.36°$ to $12.85°$ in method one, $9.84°$ in method two, $7.67°$ in method three, and $6.93°$ in method four, respectively. These results show that our methods are effective to eliminate the adverse effect of shoulder angle variations and achieve a better elbow angle estimation performance. Furthermore, this study is helpful to develop a natural and stable control system for prostheses and exoskeleton systems.

Index Terms

shoulder angle, electromyogram, elbow angle, estimation.

Z. C. Tang* is the corresponding author with the Modern Industrial Design Institute, Zhejiang University, Hangzhou 310027, China, and with the Industrial Design Institute, Zhejiang University of Technology, Hangzhou 310014, China (e-mail: ttzzcc@zju.edu.cn).

H. C. Yang, and L. K. Zhang are with the Industrial Design Institute, Zhejiang University of Technology, Hangzhou 310014, China (e-mail: yhc2016@zjut.edu.cn, zlkzhang@gmail.com).

P. C. Liu is with Lincoln Centre for Autonomous Systems, University of Lincoln, Lincoln LN5 7DH, UK (e-mail: pliu@lincoln.ac.uk).

I. INTRODUCTION

As a non-invasive technology, surface electromyogram (sEMG) signal can be used for an interaction way between people and environment efficiently and friendly in daily life [1]. Since sEMG directly shows the real-time activity level of muscles [2], [3], many previous studies applied sEMG in joint angle estimation to control the prostheses and exoskeleton systems [4], [5], [6], [7], [8], [9], [10], [11]. The overall control architecture of these applications can be generalized as: (1) preprocessing the sEMG signals to remove the noise or artifacts, (2) extracting various types of features, (3) feeding these features into a trained estimation model to identify an angle, and (4) conveying a control signal transformed from the output of the model to the device.

Most studies on sEMG-based joint angle estimation to control the prostheses and exoskeleton systems mainly aim to obtain a better off-line estimation performance according to algorithm improvement in feature extraction and estimation process [12], [13], [14], [15]. Some methods can achieve a extremely good estimation performance (higher than 95% accuracy) [16]. However, previous efforts towards sEMG-based joint angle estimation were under predefined experimental setting [17]. Some external factors, like limb position variations [18], force variations [19], [20], electrode displacements [21] and electrode locations [22], can affect the sEMG signals collection and make a worse estimation performance in practical use. Besides, the elbow angle estimation performance may be affected by the shoulder angle variations significantly. For example, in the experimental state, the arm sEMG signals are always collected at a predefined shoulder angle for each subject, which is easy to perform repeatable contractions and acquire stable training data [23]; in practical use, more unpredictable shoulder angles may happen due to the various upper-limb movements in daily life, which degrades the estimation performance deriving by physiological variations of muscles. Some researchers have turned their attention to investigate the impact of upper-limb position on performance of sEMG-based pattern recognition systems. Scheme et al. [18] used the training data and testing data from the same or different limb positions to train sEMG-based classification models, and found that limb position variations led to a significant increase of sEMG classification error from 6.9% to 35.0%. Jiang et al. [24] demonstrated that changing arm position adversely influences the prediction performance of kinematics from sEMG, and the experimental results showed the intra-position R^2 values were significantly higher than the corresponding inter-position values ($p < 0.001$). However, few studies have investigated the performance of elbow angle estimation if the shoulder angle changes.

In a traditional way, elbow angle can be estimated using sEMG signals from several arm muscles [25], [8], [26]. But since shoulder angle information cannot be acquired from sEMG of these arm muscles directly, it is difficult to deal with the adverse effect of shoulder angle using a traditional sEMG-based estimation method. The similar limitation also happens in the effect of arm position on sEMG-based gesture recognition. Several studies have focused on the additional inputs and novel estimation scheme. Geng et al. [27] used sEMG sensors and a mechanomyogram (MMG) sensor to solve the effect of limb position on motion classification for real-time prostheses control, and achieved a maximum increase of completion rate from 81.4% to 94.3%. Park et al. [28] applied the ensemble-learning method to propose a position-independent decoding model to estimate the likelihood of different arm positions, which could successfully decode four wrist movements in different arm positions. In addition, not many efforts aimed to solve the effect of shoulder angle on elbow angle estimation. Fougner et al. [23] used sEMG sensors and two accelerometers to eliminate the effect of arm position and shoulder angle on sEMG pattern recognition, but like most previous studies, this study mainly focused on different arm positions (only three different shoulder angle were considered). Boschmann et al. [29] applied a high density electrode array to reduce the shoulder angle effect in distinguishing different hand and wrist movements, but this method using an electrode array (including 96 sEMG sensors) cost too much.

In this paper, we firstly evaluate the adverse effect of shoulder angle variations on elbow angle estimation. For solving this problem, we propose four methods:

1) Method one: using a training set including all shoulder angles' training data to train model.
2) Method two: adding two shoulder muscles's sEMG as additional inputs. Shoulder angle value can be estimated by shoulder muscles's sEMG. This lets the estimation model include more kinds of training data, and increases the input vectors' space dimensionality.
3) Method three: a two-step method using arm muscles' sEMG and two shoulder muscles' sEMG. There are two steps in this method: in step 1, the shoulder muscles' sEMG data are classified to get a specific shoulder angle; in step 2, the corresponding pre-trained model in the evaluation stage using the same shoulder angle's training data is used for elbow angle estimation.
4) Method four: a two-step method using arm muscles' sEMG and measured shoulder angle

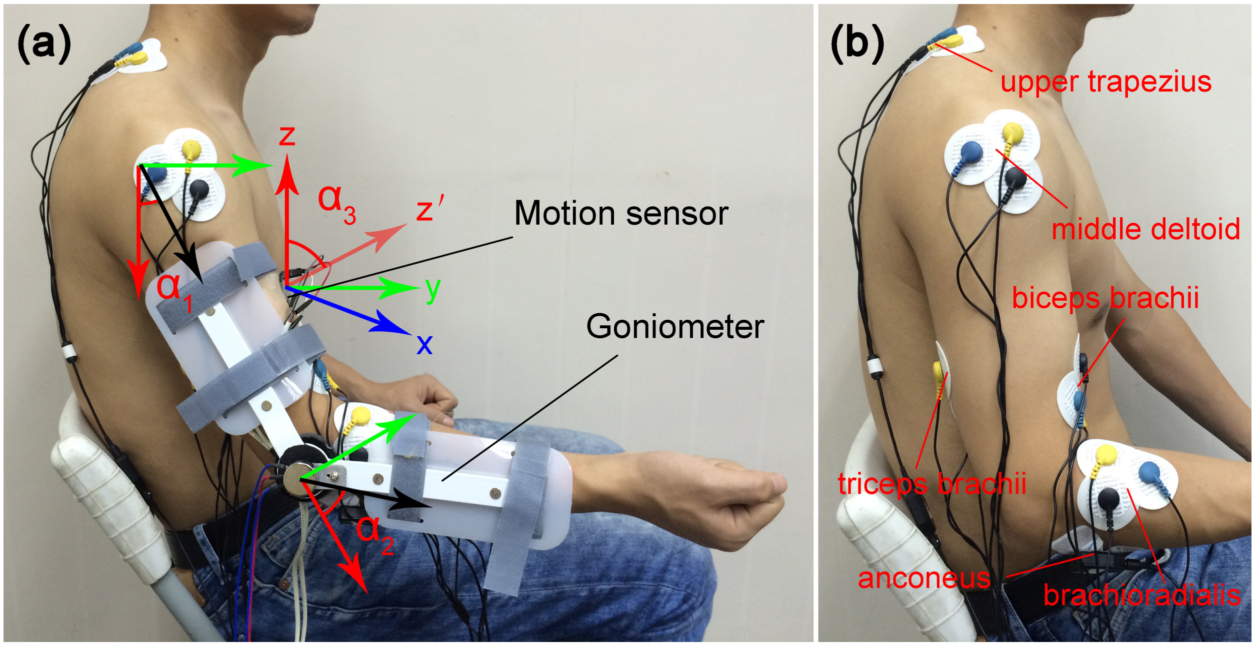

Fig. 1. Experimental setup (a) and electrode position (b). Shoulder angle is represented by α_1. Elbow angle is represented by α_2. The angle between motion sensor's z-axis and natural coordinates' z-axis is represented by α_3. The motion sensor was used to measure the shoulder angle in Method four, which was placed about 10cm from the elbow joint on the midline of the upper arm. The goniometer was made by ourselves to acquire the actual elbow angle. It consists of a potentiometer, two metal bars, a rotation axis and four belts.

value by a motion sensor. There are two steps in this method: in step 1, the motion sensor data are classified to get a specific shoulder angle; in step 2, the corresponding pre-trained model in the evaluation stage using the same shoulder angle's training data is used for elbow angle estimation.

II. Methods

A. Subjects

13 male able-bodied subjects (age range: 26±3 years, height range: 172±6cm, weight range: 65±5kg) were volunteered to participate in our experiment. The ethical committee of Zhejiang University reviewed our experimental protocol and approved it. All subjects were informed not to perform any intense movements to avoid fatigue on the day of experiment, and they all signed the informed consents prior to the experiment.

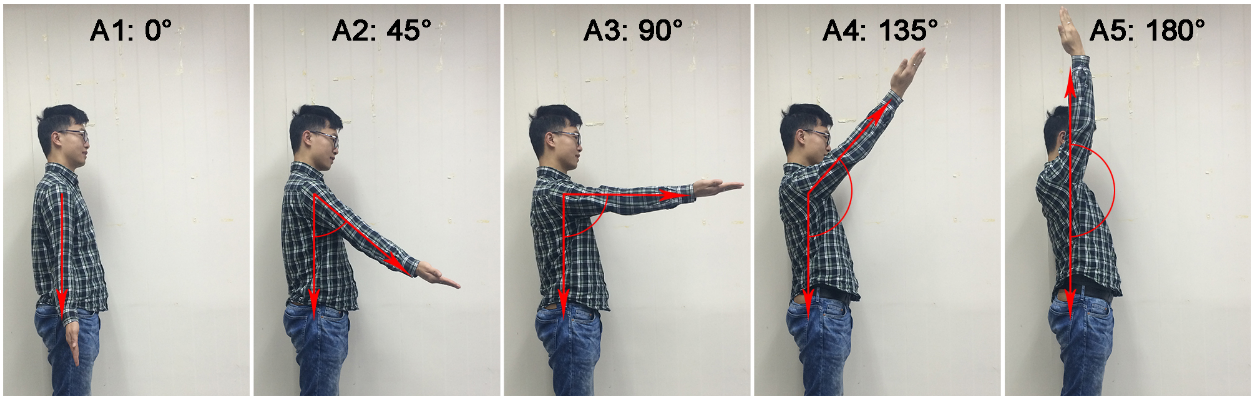

Fig. 2. Five different shoulder angles (α_1) in the sagittal plane, i.e., 0°, 45°, 90°, 135° and 180°, respectively.

TABLE I
THE DIFFERENT CONDITIONS IN TEN TRIALS

Trial	Shoulder angle	Speed
Run1	A1:0°	V1: constant elbow angular velocity of 90°/s (0.5Hz)
Run2	A1:0°	V2: constant elbow angular velocity of 45°/s (0.25Hz)
Run3	A2:45°	V1: constant elbow angular velocity of 90°/s (0.5Hz)
Run4	A2:45°	V2: constant elbow angular velocity of 45°/s (0.25Hz)
Run5	A3:90°	V1: constant elbow angular velocity of 90°/s (0.5Hz)
Run6	A3:90°	V2: constant elbow angular velocity of 45°/s (0.25Hz)
Run7	A4:135°	V1: constant elbow angular velocity of 90°/s (0.5Hz)
Run8	A4:135°	V2: constant elbow angular velocity of 45°/s (0.25Hz)
Run9	A5:180°	V1: constant elbow angular velocity of 90°/s (0.5Hz)
Run10	A5:180°	V2: constant elbow angular velocity of 45°/s (0.25Hz)

B. Experimental Procedure

When subjects arrived, one experimenter helped them attach the sensors (sEMG sensors, motion sensor and goniometer) on the right arm and ensured that the signals were normal according to the signal check procedures from Konrad [30]. The signal check procedures included the skin impedance test (impedance range keeps in 1-5Kohm) and the visual inspection of the raw EMG baseline (the average noise level should be located at 1-3.5 microvolts, and the baseline should remain at the zero line). Then, subjects sit on a chair to perform flexion-extension movements of elbow in the sagittal plane (Fig. 1(a)). The elbow angle range (α_2) was from $0°$ to $90°$. $0°$ represented full extension, and $90°$ represented full flexion. The forearm was supinated throughout the experiment.

During the experiment, the subjects performed flexion-extension movements of elbow under five different shoulder angles (α_1) in the sagittal plane, i.e., $0°$, $45°$, $90°$, $135°$ and $180°$, respectively (as shown in Fig. 2). For each shoulder angle, subjects performed sixty trials (one flexion-extension movement is called a trial) continuously at two speeds. Each subject needed to perform ten runs under different shoulder angles and speeds (Table I), forming a total dataset of 60 trials $\times$ 5 shoulder angles $\times$ 2 speeds $\times$ 13 subjects. For each trial, the arm and elbow moved smoothly in a constant speed, and no delay at two ends ($0°$ to $90°$). Subjects followed the beeps of a metronome to perform the elbow movements at different speeds [31], and finished one trial between two beeps.

There was a resting period of 4-6 minutes between two runs to avoid fatigue. If subjects felt too fatigued to continue the flexion-extension movements during one run, they could stop the experiment and have a rest. Besides, one experimenter watched the targeted muscles' median frequency (MF) during the experiment. Muscle fatigue can result in a decline of MF [32], [33]. The two measures were effective to avoid fatigue for all sEMG records. The whole experiment lasted about 70 minutes per subject.

C. Data Acquisition

To estimate the elbow angle in this experiment, sEMG signals were collected from four arm muscles (biceps brachii, triceps brachii, brachioradialis and anconeus). Biceps brachii and triceps brachii are the agonistic muscles in elbow flexion movement and extension movement, respectively; brachioradialis and anconeus are the synergistic muscles in elbow flexion movement and extension movement, respectively [34]. To estimate the shoulder angle in Method two and Method three, sEMG signals were collected from two shoulder muscles, i.e., middle deltoid and upper trapezius [35], [36]. These four muscles' sEMG signals were collected by four EMG MyoScan-Z sensors (T9503Z, Thought Technology Ltd., Canada). The sensor measures raw sEMG signals with a range from 0 up to 2000μV. Input impedance is greater than 10GΩ in parallel with 10pF, CMRR is greater than 130dB, and input/output gain equals 500. Before attaching the electrodes, we used alcohol and conductive gel to clean the skin and improve the contact between electrodes and skin [30], respectively. Then, the electrodes of the sEMG sensors were placed on the targeted muscles of the right arm for each subject. One sensor included three electrodes: positive, negative and ground. The inter-electrode distance was 2cm. The electrode position is shown in Fig. 1(b). sEMG signals were sampled at 1024Hz and were filtered at 5-350Hz with a band-pass filter. And a 50-Hz notch filter was applied to remove the power-line interference.

One motion sensor with a 3-axis accelerometer and 3-axis gyroscope (MPU6050, InvenSense Inc., California) was used to measure the shoulder angle variation in Method four. For this sensor, the range of angular velocity is $\pm 2000°$/s, and the range of acceleration is ± 16g. The placement of the motion sensor is shown in Fig. 1(a). The angular velocity data are given by a 16-bit analog-to-digital converter in motion sensor, and then the angular acceleration data are obtained by

$$Acc = \lim_{\Delta t \to 0} \frac{\Delta \omega}{\Delta t} \tag{1}$$

where $\Delta\omega$ is angular velocity's change in one time interval of Δt. The shoulder angle α_1 is calculated by

$$\alpha_1 = \alpha_3 + 90° = \tan^{-1}\left(\frac{\sqrt{Acc_x^2 + Acc_y^2}}{Acc_z}\right) + 90° \tag{2}$$

where α_3 represents the angle between motion sensor's z-axis and natural coordinates' z-axis, Acc_x is the angle acceleration of motion sensor's x-axis, Acc_y is the angle acceleration of motion sensor's y-axis, and Acc_z is the angle acceleration of motion sensor's z-axis. The range of α_1 is from $0°$ to $180°$, and the range of α_3 is from $-90°$ to $+90°$.

One goniometer made by ourselves wearing on the subject's right arm was applied to collect the elbow angle' actual value to compare with the predicted value. The structure of this goniometer referred to some previous studies ([37], [38], [8]), including a potentiometer (RV30YN30S, TOCOS, Japan), two metal bars, a rotation axis and four belts. The shaft of the potentiometer is fixed on the rotation axis. When the rotation axis moves in one angle, the potentiometer's shaft moves in a same angle, resulting in an output of the corresponding voltage [39]. The actual elbow angle α_2 can be calculated by

$$\alpha_2 = \frac{U_{out}}{U_{max}} \theta_{max} \tag{3}$$

where U_{out} is the output voltage, U_{max} is the input voltage, and θ_{max} is the maximum angle which the shaft of the potentiometer can move. According to the testing, the angle range is $0 - 120°$, and the accuracy is $0.1°$. To avoid affecting the natural arm movement, the four flexible belts are adjustable to match different subjects. The light weight of the goniometer (0.185kg) minimizes the effect on the EMG signals as much as possible.

To synchronize with the sEMG data, all angle data were sampled at 1024Hz.

D. Feature Extraction

To extract features from all data, they were segmented by an overlapped windowing technique [40]. Each time window had a length of 50ms and was overlapped by 25ms.

Many time-domain methods of feature extraction were developed for sEMG-based applications [41], [42]. Four of them, i.e., root mean square (RMS), zero crossing (ZC), mean absolute value (MAV) and waveform length (WL), were utilized in our study. RMS provides the amplitude information of sEMG signals. It can be calculated by

$$RMS = \sqrt{\frac{1}{N}\sum_{i=1}^{N} X_i^2} \tag{4}$$

where X_i is the ith sEMG signal value and N is the number of time points. MAV stands for the signal energy as below

$$MAV = \frac{1}{N}\sum_{i=1}^{N} |X_i| \tag{5}$$

ZC is the total zero crossing times occurring in a time window, which can describe the frequency characteristic in time domain. It is presented in

$$ZC = \sum_{i=1}^{N-1} \phi(\Delta_i) \tag{6}$$

$$\phi(\Delta_i) = \begin{cases} 1 & \text{if } X_i \times X_{i+1} < 0 \text{ and } |X_i - X_{i+1}| \geq ZC_{threshold} \\ 0 & \text{otherwise} \end{cases} \tag{7}$$

where $ZC_{threshold}$ is a threshold to reduce noises caused by zero crossings in calculation. WL represents the waveform complexity of the sEMG signals, which can be calculated by

$$WL = \sum_{i=1}^{N} [X_i - X_{i-1}] \tag{8}$$

In each time window, the shoulder angle from the motion sensor and the elbow angle from the goniometer were averaged by

$$\overline{\alpha_1} = \frac{1}{N} \sum_{i=1}^{N} (\alpha_1)_i \tag{9}$$

$$\overline{\alpha_2} = \frac{1}{N} \sum_{i=1}^{N} (\alpha_2)_i \tag{10}$$

where $\overline{\alpha_1}$ is the average shoulder angle, $\overline{\alpha_2}$ is the average elbow angle, $(\alpha_1)_i$ is the ith shoulder angle value and $(\alpha_2)_i$ is the ith elbow angle value.

E. Estimation

Support vector regression (SVR) can transform the training data into a high-dimension feature space [43]. It was used to learn the mapping model between sEMG and elbow angle in this study. The inputs of SVR model were sEMG features, and the output of SVR model was corresponding elbow angle. The radial based function (RBF) was used in model training as the kernel function to map the input x into a higher dimensional space:

$$K(x, x_i) = exp\left(-\frac{1}{2\sigma^2} \left\|x - x_i\right\|^2\right) \tag{11}$$

where σ is the scale factor, and exp is the exponential function. After the model training, the sEMG-angle mapping model was constructed.

In the evaluation stage, to demonstrate the effect of shoulder angle variation on elbow angle estimation performance, we trained the SVR models using data from one shoulder angle and tested in all shoulder angles under each speed (totally ten models for each subject). The inputs of SVR models were sEMG features of four arm muscles, and the output was corresponding elbow angle. For all models, 80% data were selected randomly as training data for model training, and 20% data were utilized as testing data for model testing. In model training, the training data were separated into ten folds (9 folds for training and 1 fold for testing) to perform 10-fold

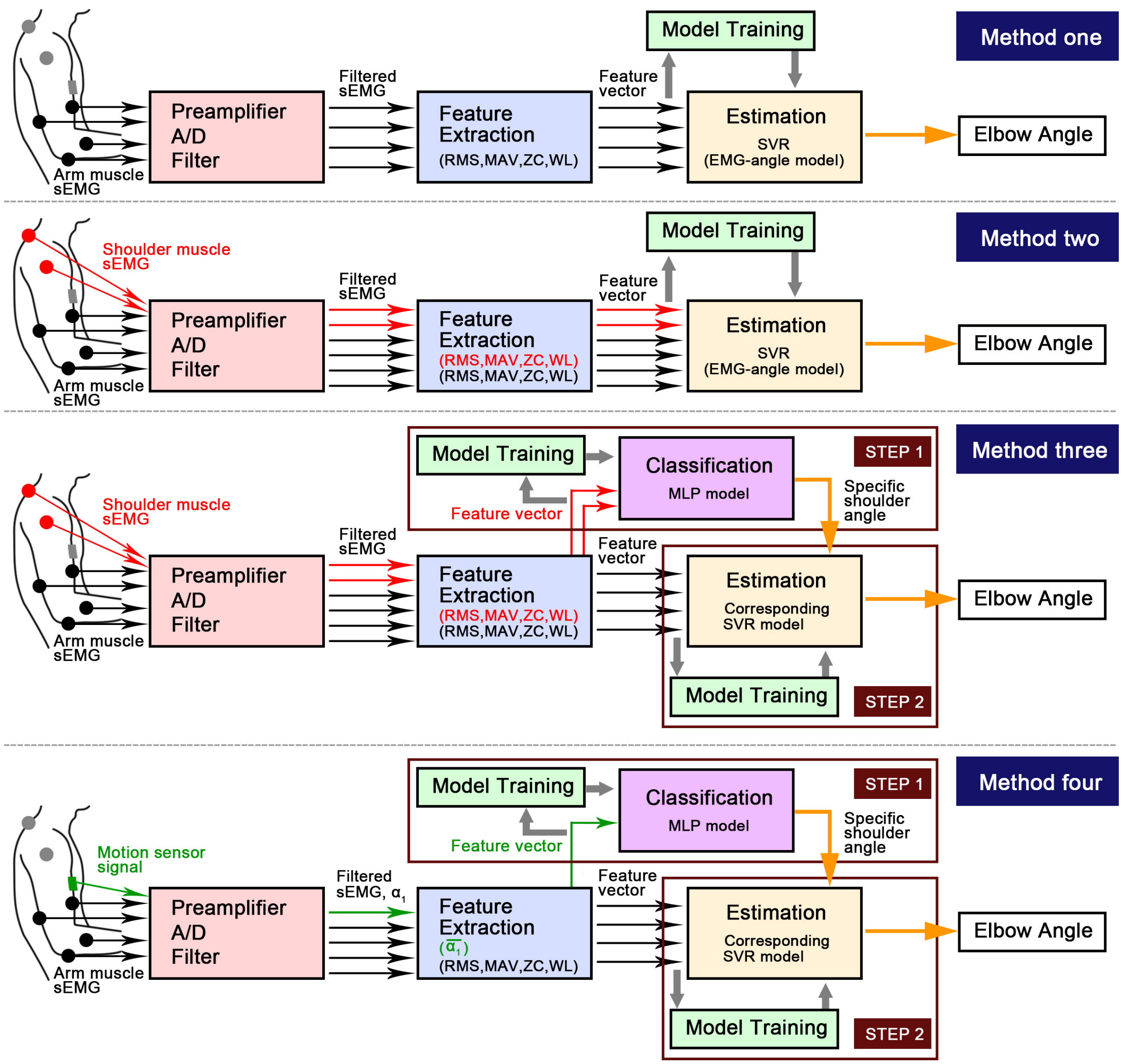

Fig. 3. The estimation scheme of four proposed methods. Method One: using a training set including all shoulder angles' training data; Method two: adding two shoulder muscles's sEMG as additional inputs; Method three: a two-step method using arm muscles' sEMG and two shoulder muscles' sEMG; Method four: a two-step method using arm muscles' sEMG and measured shoulder angle value by a motion sensor.

cross-validation. For each speed, intra-angle estimation performance (training and testing data from one same shoulder angle) and inter-angle estimation performance (training and testing data from different shoulder angles) were evaluated.

For resolving the effect of shoulder angle variation, we proposed the following four methods (as shown in Fig. 3):

1) Method One - using a training set including all shoulder angles' training data: Under each speed, the inputs of SVR models were four arm muscles' sEMG, and the output was corresponding elbow angle. A training set including all five shoulder angles' training data (randomly 80% data) was used for SVR model training. A testing set including all five shoulder angles' testing data (remaining 20% data) was used for SVR model testing. 10-fold cross-validation was used in model training.

2) Method Two - adding two shoulder muscles's sEMG as additional inputs: Shoulder muscles's sEMG can estimate the shoulder angle, which increases the space dimensionality of estimation algorithm. Under each speed, the inputs of SVR models were four arm muscles' sEMG and two shoulder muscles' sEMG, resulting in a feature vector:

$$\left\{\begin{matrix} [(RMS_j)_N, (MAV_j)_N, (ZC_j)_N, (WL_j)_N]_{arm}, j = 1...4 \\ [(RMS_k)_N, (MAV_k)_N, (ZC_k)_N, (WL_k)_N]_{shoulder}, k = 1...2 \end{matrix}\right\} \tag{12}$$

where j and k are the number of electrodes, and N is the number of time points. The output was the corresponding elbow angle. A training set including all five shoulder angles' training data (randomly 80% data) was used for SVR model training. A testing set including all five shoulder angles' testing data (remaining 20% data) was used for SVR model testing. 10-fold cross-validation was used in model training.

3) Method Three - a two-step method using arm muscles' sEMG and two shoulder muscles' sEMG: Under each speed, in step 1, shoulder muscles' sEMG were classified to recognize a specific shoulder angle ($0°$, $45°$, $90°$, $135°$ and $180°$). Multi-Layer perceptron neural network (MLP) was used to the classifier in this step due to its good robustness and performance in extensive sEMG-based applications [44]. MLP can learn nonlinear functions through weights adjusting to minimize the output error. A training set including all five shoulder angles' training data (randomly 80% data) was used for the training of MLP classifier. A testing set including all five shoulder angles' testing data (remaining 20% data) was used for the testing of MLP classifier. 10-fold cross-validation was used in model training. After the model training, we obtained a specific shoulder angle from the shoulder muscles' sEMG. In step 2, the corresponding pre-trained model in the evaluation stage using the same shoulder angle's training data was used for elbow angle estimation.

4) Method Four - a two-step method using arm muscles' sEMG and measured shoulder angle value by a motion sensor: Under each speed, in step 1, motion sensor data were classified to recognize a specific shoulder angle ($0°$, $45°$, $90°$, $135°$ and $180°$) using an MLP classifier. A training set including all five shoulder angles' training data (randomly 80% data) was used for the training of MLP classifier. A testing set including all five shoulder angles' testing data (remaining 20% data) was used for the testing of MLP classifier. 10-fold cross-validation was used in model training. After the model training, we obtained a specific shoulder angle from the motion sensor data. In step 2, the corresponding pre-trained model in the evaluation stage using the same shoulder angle's training data was used for elbow angle estimation.

We used root mean square (RMS) error to evaluate the estimation performance of SVR models of evaluation stage and four methods. The RMS error between predicted angle and actual angle can be obtained by

$$RMSE_m = \sqrt{\frac{1}{n}\sum_{m=1}^{n}[(\alpha_2')_m - (\alpha_2)_m]^2} \tag{13}$$

where n is the number of testing data, $(\alpha_2')_m$ is the predicted angle, and $(\alpha_2)_m$ is the actual angle. Then, we used the relative magnitude of the angle error to the actual angle to compare the four methods further. The relative magnitude ($\%error$) can be calculated by

$$\%error_m = \frac{1}{n}\sum_{m=1}^{n}\left(\frac{\left|(\alpha_2')_m - (\alpha_2)_m\right|}{(\alpha_2)_m}\right) \tag{14}$$

III. Results

All data of 13 subjects were processed using MATLAB (MathWorks, Inc., USA). The sEMG and actual angle of one flexion-extension trial from five shoulder angles of one subject at V1 are shown in Fig. 4. A one-way ANOVA with a 0.05 significance level was used to evaluate the shoulder angle main effect on muscles' sEMG. There is a significant main effect of shoulder angle for the sEMG of biceps brachii ($F = 7.364, p = 0.004$), triceps brachii ($F = 6.588, p = 0.011$), anconeus ($F = 2.946, p = 0.041$), middle deltoid ($F = 4.226, p = 0.027$) and upper trapezius ($F = 6.782, p = 0.009$). To further clarify this effect, the Tukey post-hoc test was applied and shows that A1 ($0°$) is significantly different from the other four shoulder angles for the sEMG of these six muscles (all $p < 0.05$). The sEMG of arm muscles and shoulder muscles are changed with the change of the shoulder angle, i.e., the increase of the shoulder angle results in the amplitude decrease of biceps brachii and the amplitude increase of triceps brachii, anconeus,

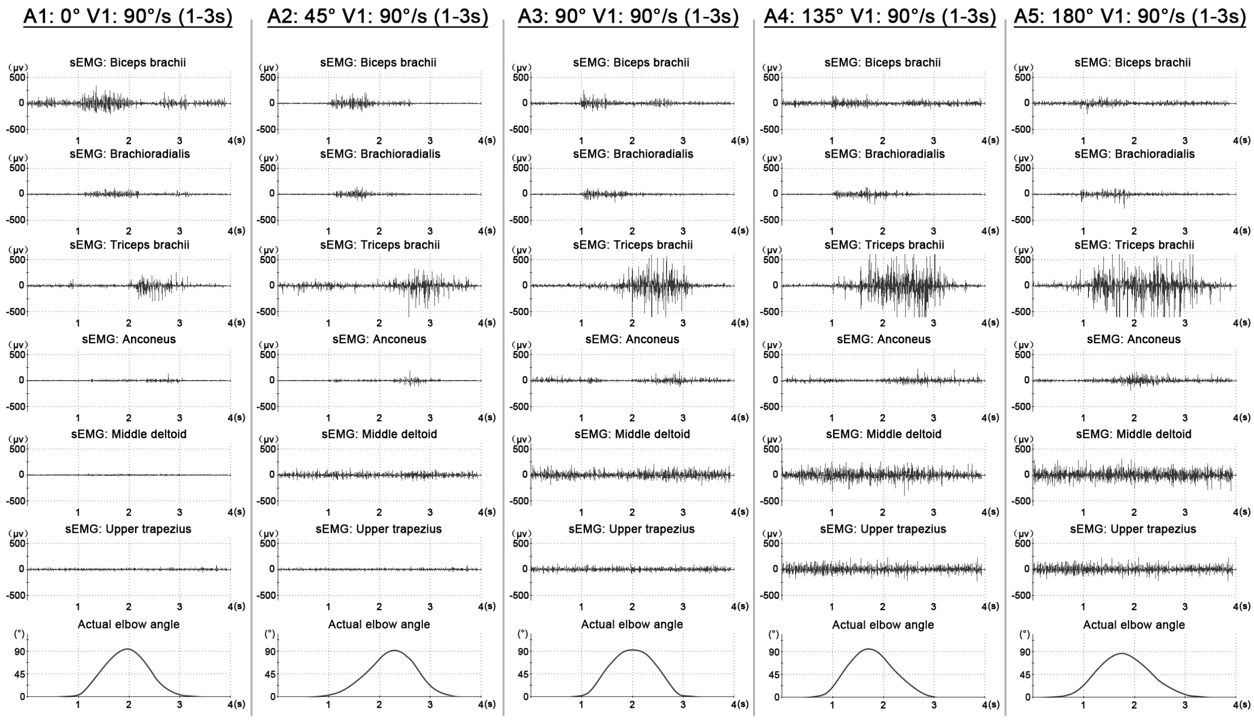

Fig. 4. The sEMG and actual elbow angle of one flexion-extension trial from five shoulder angles of one subject at V1 (90°/s).

middle deltoid and upper trapezius. There is no significant main effect of shoulder angle for the sEMG of Brachioradialis ($F = 0.952, p = 0.138$). Brachioradialis has no obvious change across five shoulder angles.

A. Results in Evaluation Stage

Totally ten different shoulder angle-specific SVR models (5 shoulder angles $\times$ 2 speeds) were trained for each subject. For each model, the training data were from one shoulder angle, and the testing data were from all shoulder angles. The results (confusion matrix) are shown in Fig. 5(a). The value of each entry in confusion matrix stands for the RMS error (mean$\pm$sd) of the corresponding training shoulder angle (vertical axis) and testing shoulder angle (horizontal axis) across all subjects and speeds. Darker color indicates larger RMS error. The RMS errors of the main diagonal represent the intra-angle cases (training and testing data from one same shoulder angle), and the RMS errors of the off-diagonal represent the inter-angle cases (training and testing data from different shoulder angles). For each training shoulder angle (each row of the confusion matrix), a one-way ANOVA with a 0.05 significance level was used to evaluate the main effect of

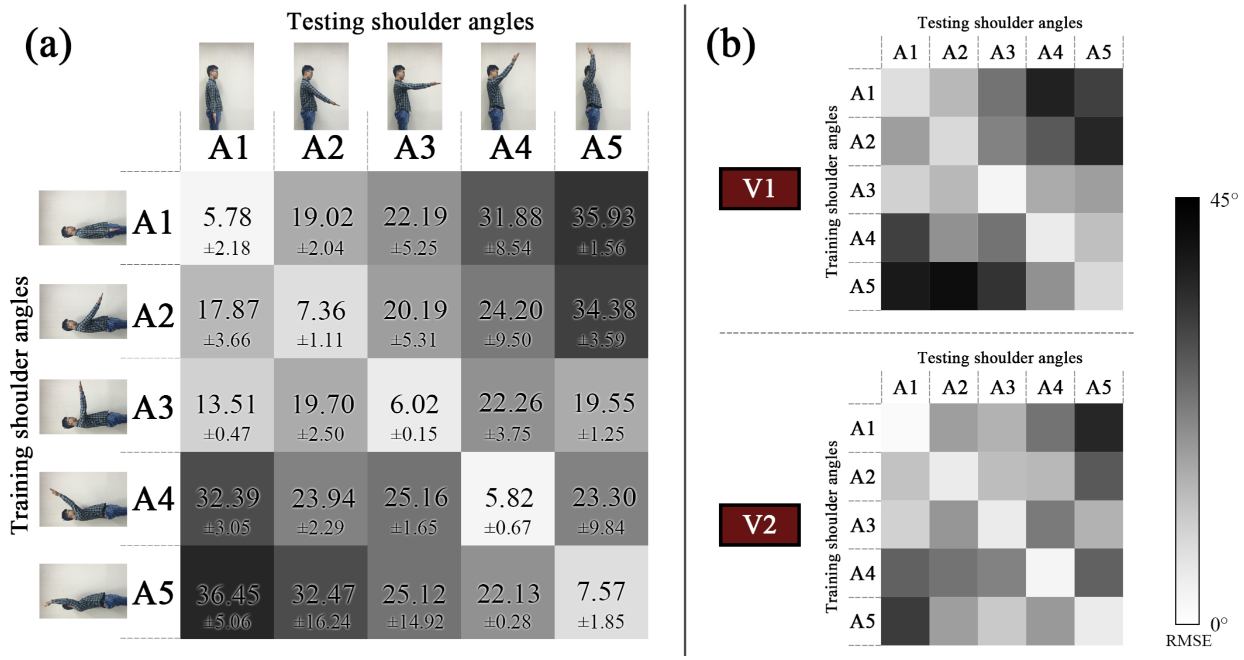

Fig. 5. RMS error (mean±sd°) resulting matrices. Darker color indicates larger RMS error. (a): the value of each entry in confusion matrix stands for the RMS error (mean±sd°) of the corresponding training shoulder angle (vertical axis) and testing shoulder angle (horizontal axis) across all subjects and speeds; (b): speed specific matrices broken out from (a).

shoulder angle variation on elbow angle estimation performance, resulting in totally 5 ANOVAs. Each ANOVA includes 5 levels, i.e., one intra-angle case and four inter-angle cases. There is a significant main effect of shoulder angle variation on elbow angle estimation performance for all ANOVAs (($F = 10.532, p = 0.001$), ($F = 7.043, p = 0.008$), ($F = 4.376, p = 0.020$), ($F = 7.643, p = 0.006$) and ($F = 9.890, p = 0.002$), respectively). The Tukey post-hoc test was applied and shows that the intra-angle case is significantly different from the inter-angle cases for all ANOVAs (all $p < 0.05$). In A1 ANOVA, A1-A5 is significantly different from the other cases (all $p < 0.05$); in A2 ANOVA, A2-A5 is significantly different from the other cases (all $p < 0.05$); in A4 ANOVA, A4-A1 is significantly different from the other cases (all $p < 0.05$); in A5 ANOVA, A5-A1 is significantly different from the other cases (all $p < 0.05$). As shown in the matrix, training data from A5 and testing data from A1 or vice versa leads to the poorest results ($36.45°$ and $35.93°$, respectively). Similarly, the results of A1-A4, A4-A1, A2-A5 and A5-A2 ($31.88°$, $32.39°$, $34.38°$ and $32.47°$, respectively) are poor as well, although better than A5-A1 and A1-A5. In addition, if the difference between training shoulder angle and testing shoulder angle is larger, the estimation performance is poorer, e.g., the RMS errors gradually

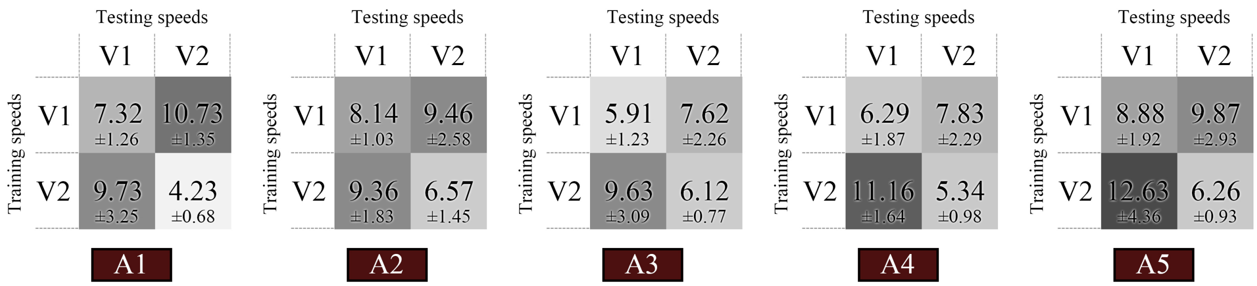

Fig. 6. RMS error (mean±sd°) resulting matrices under five shoulder angles. Darker color indicates larger RMS error. The value of each entry in five matrices stands for the RMS error (mean±sd°) of the corresponding training speed (vertical axis) and testing speed (horizontal axis) across all subjects.

increase from A1-A1 to A1-A5. The mean intra-angle RMS error is $6.51°$, which is much lower than the mean inter-angle RMS error ($22.02°$) and the mean overall RMS error ($21.36°$). This adverse effect increases mean RMS error by $14.85°$ between mean intra-angle RMS error and mean overall RMS error.

To further demonstrate the shoulder angle effect on elbow angle estimation under different speeds, two speed specific matrices stemming from the matrix of Fig. 5(a) are shown in Fig. 5(b). Fig. 6 illustrates the similar resulting matrices as those in Fig. 5(b), but the value of each entry in five matrices stands for the RMS error (mean±sd) of the corresponding training speed (vertical axis) and testing speed (horizontal axis) across all subjects. Fig. 5(b) and Fig. 6 show the effect of different speeds on the elbow joint estimation performance. There is a significant difference ($p < 0.05$) between two speed matrices in Fig. 5(b) through the t-test with a 0.05 significance level, and the color of entries under V1 is darker than those under V2. The RMS errors of inter-speed are larger than those of intra-speed in five matrices shown in Fig. 6 (the total mean inter-angle RMS error is $9.80°$ and the total mean intra-angle RMS error is $6.51°$).

B. Results in Four Methods

In Method one, a training set including all shoulder angles' training data was used to train model. We built different training combinations with training data of different shoulder angles into five groups to analyze the effect of the amount of training data on estimation performance. For each group, the estimation model was trained by training data from different amount of shoulder angles (one, two, three, four or five), and was tested by testing data from all five shoulder angles. All groups' mean RMS errors at two speeds across all subjects are shown in

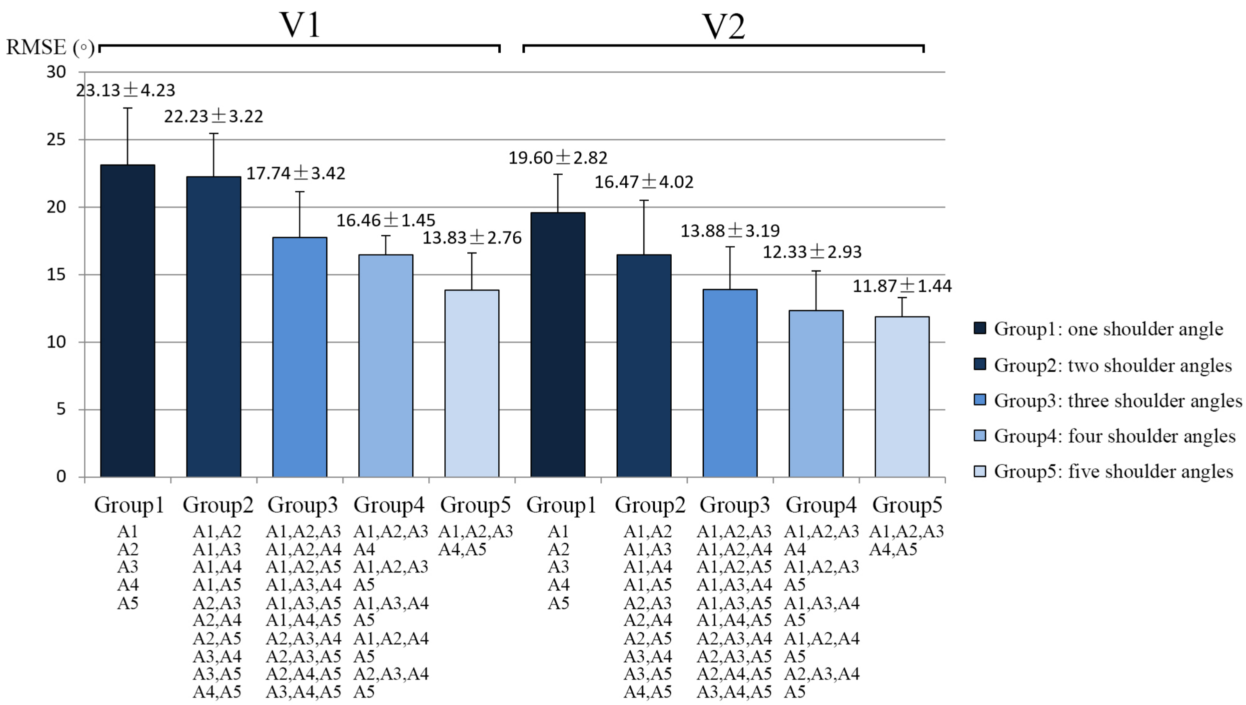

Fig. 7. All groups' mean RMS errors at two speeds across all subjects. For each group, the estimation model was trained by training data from different amount of shoulder angles (one, two, three, four or five), and was tested by testing data from all five shoulder angles.

Fig. 7. For each speed, a one-way ANOVA with a 0.05 significance level was used to evaluate the main effect of the amount of training data on estimation performance. There is a significant main effect of the amount of training data on elbow angle estimation performance for two ANOVAs (($F = 3.243, p = 0.039$) and ($F = 2.842, p = 0.044$), respectively). The mean RMS error decreases gradually from Group 1 trained by one shoulder angle to Group 5 trained by five shoulder angles at each speed. This result demonstrates that adding more training data from different shoulder angles can lead to a better estimation performance. The SVR model of Group 1 (training data from one shoulder angle) has a poorest estimation performance.

In Method two, two shoulder muscles' sEMG were used as additional inputs for the SVR models. In the step 1 of Method three and Method four, under each speed, the two shoulder muscles' sEMG and the motion sensor data were classified to get a specific shoulder angle, respectively. By using an MLP classifier, the shoulder angle classification error was 3.3% in Mehthod three and 0% in Method four. Then, the corresponding pre-trained model in the eval-

TABLE II
THE RMS ERRORS (MEAN±SD°) OF FOUR METHODS AT TWO SPEEDS ACROSS ALL SUBJECTS

	Method one (mean±sd)	Method two (mean±sd)	Method three (mean±sd)	Method four (mean±sd)
V1	13.83 ± 1.20	9.96 ± 1.33	8.31 ± 1.93	8.01 ± 1.83
V2	11.87 ± 1.15	9.71 ± 2.01	7.03 ± 1.44	5.84 ± 0.93
Total	12.85 ± 1.39	9.84 ± 1.89	7.67 ± 0.91	6.93 ± 1.53

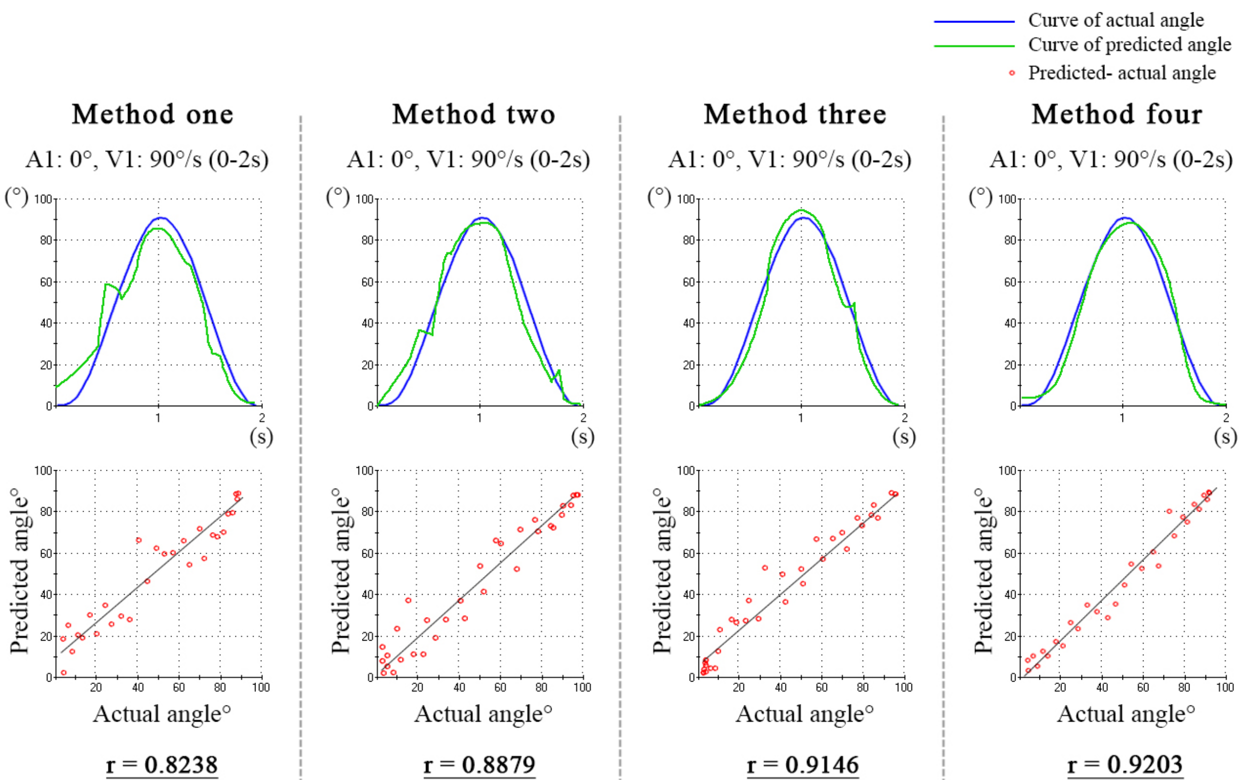

Fig. 8. The curves of predicted and actual angle, the value of r and the correlation diagram of four methods using testing data of one same flexion-extension trial at V1 and A1 from one subject.

uation stage using the same shoulder angle's training data was used for elbow angle estimation in step 2 of the two methods. Table II shows the mean RMS error of the four methods at two speeds. Fig. 8 shows the curves of predicted and actual angle, the correlation diagram and the values of Pearson correlation coefficient (r) of four methods using testing data of one same flexion-extension trial at V1 and A1 from one subject. If r is closer to 1, it means the error between predicted and actual angle is smaller. According to Table II and Fig. 8, we find that

TABLE III
THE $\%errors$ (MEAN±SD%) OF FOUR METHODS AT FIVE SHOULDER ANGLES AND TWO SPEEDS ACROSS ALL SUBJECTS

		Method one (mean±sd)	Method two (mean±sd)	Method three (mean±sd)	Method four (mean±sd)
V1	A1	24.68 ± 1.43	16.25 ± 4.93	12.65 ± 1.73	11.87 ± 2.33
	A2	21.50 ± 3.34	15.93 ± 1.29	12.08 ± 1.30	11.99 ± 2.87
	A3	23.85 ± 3.98	17.48 ± 3.81	12.83 ± 4.33	12.98 ± 1.99
	A4	23.60 ± 2.43	14.31 ± 2.43	11.15 ± 4.09	11.31 ± 1.73
	A5	24.20 ± 5.22	18.11 ± 1.43	11.34 ± 3.24	13.55 ± 3.99
V2	A1	23.16 ± 3.95	17.46 ± 2.76	12.81 ± 2.30	10.46 ± 3.54
	A2	22.58 ± 4.32	18.36 ± 5.17	13.71 ± 2.48	12.93 ± 3.42
	A3	21.56 ± 2.04	16.31 ± 3.89	11.13 ± 2.98	11.34 ± 3.28
	A4	20.81 ± 2.76	16.13 ± 3.41	10.98 ± 1.79	11.31 ± 2.95
	A5	25.04 ± 3.02	17.75 ± 4.03	11.63 ± 3.44	12.14 ± 2.55
Total		23.09 ± 1.44	16.81 ± 1.24	12.03 ± 0.93	11.96 ± 0.91

Method four achieves a better estimation performance (mean RMS error at V1, mean RMS error at V2, total mean RMS error and the value of r are $8.01°$, $5.84°$, $6.93°$ and 0.9203 respectively) than the other three. Additionally, four methods' RMS errors are all lower than evaluation stage's RMS error $(21.36°)$ using training data from one single shoulder angle and testing data from all shoulder angles. According to the t-test with a 0.05 significance level, all methods' RMS errors have a significantly difference with evaluation stage's RMS error (all $p < 0.05$).

Furtherly, we used the relative magnitude ($\%error$) of the angle error to the actual angle to compare the four methods. If $\%error$ is closer to 0, it means the predicted angle is closer to the actual angle. The $\%error$s (mean±sd) of four methods at five shoulder angles and two speeds across all subjects are shown in Table III. For four methods, the results of $\%error$ are similar to those of RMS error. Method four has a lower total mean $\%error$ (11.96%) than the other three, which means that Method four achieves a best estimation performance. Method three has a slightly higher total mean $\%error$ (12.03%), which is very close to Method four.

IV. DISCUSSION

To evaluate the effect of shoulder angle variation on elbow angle estimation performance, we trained estimation models using training data from one shoulder angle and tested them using testing data from all shoulder angles. Fig. 5(a) shows that the mean intra-angle RMS error ($6.51°$) using training and testing data from one same shoulder angle is much lower than the mean inter-angle RMS error ($22.02°$) using training and testing data from different shoulder angles. This result implies that shoulder angle variations can affect the elbow angle estimation substantially. The possible reasons of this fact are: (1) Variation in muscle recruitment. When arm is stabilized in a specific shoulder angle, this will lead to the displacement of muscles due to different force of gravity, and alter the nature of the sEMG of arm muscles [16]. (2) Electrode shift. The electrodes may shift during use because of the changes in muscle shape, length and position [23]. Hargrove et al. [45] found a 1-cm shift of four electrodes attached on the arm caused an increase of classification error from 5% to 40%. And (3) the change of the lever arm of musculotendon and the change of the muscle's force-length relationship [23]. Therefore, training the control system of a prosthesis or exoskeleton using data from a single shoulder angle is insufficient due to the requirement in complex movements in daily life. Shoulder angle variation can induce a significant difference between the experiment in the laboratory and practical use. The ideal conditions (predefined experimental setting) will not always happen in practical use.

To solve this problem, we proposed four methods in our study. In Method one, the total mean overall RMS error is reduced from $21.36°$ to $12.85°$ according to use a training set including all shoulder angles' training data. Using training data from multiple shoulder angles to train model will require more time for collecting training data. For example, according to the experimental procedure of this study, if we add the training data of another angle, each subject needs add about 11 minutes (60 trials $\times$ 2 speeds $\times$ 3 second (average movement time per trial) $+$ 5 minutes (average resting time per run)). Therefore, we hope to use the training data from as few shoulder angles as possible. However, the mean RMS error increases along with the reduction of shoulder angles (from Group5 to Group1) at each speed. This result shows that adding more training data from different shoulder angles can lead to a better estimation performance. The SVR model of Group 1 (training data from one shoulder angle) has a poorest estimation performance. In Method two, the total mean overall RMS error is reduced from $21.36°$

to $9.84°$ by using two shoulder muscles' sEMG as additional inputs for the SVR models. The better estimation performance in Method two than in Method one is because additional inputs increases the input vectors' space dimensionality. In step 1 of Method three and Method four, the two shoulder muscles' sEMG and the motion sensor data were classified to get a specific shoulder angle, respectively. Then, the corresponding pre-trained model in the evaluation stage using the same shoulder angle's training data was used for elbow angle estimation in step 2 of the two methods. A further reduction of the total mean RMS error of two methods is from $9.84°$ to $7.67°$ and to $6.93°$, respectively. Additionally, these two methods have a lower total mean $\%error$ (12.03% and 11.96%, respectively) than Method two. These results show that Method three and Method four have a better estimation performance than Method two. The reason is that the estimation performance of Method two is still influenced by inter-angle cases (testing data from different shoulder angles). In Method three and four, because of the nearly zero (3.3%) and zero classification error in step 1, the estimation process in step 2 is same as the intra-angle cases resulting in a much lower mean RMS error than that of the inter-angle cases. The better estimation performance in Method four than in Method three indicates that, to classify the shoulder angle, using a motion sensor is better than using shoulder muscles' sEMG. That is because shoulder muscles' sEMG also can be affected by variation in muscle recruitment and electrode shift in different movements like arm muscles' sEMG. The estimation performance of all four methods is better than that of evaluation stage. To compare with the first three methods which only use sEMG data to train model, Method four based on sensor fusion technology (sEMG and motion sensor) has a better estimation performance.

Additionally, the effect of different speeds on elbow angle estimation performance is found. As shown in Fig. 5(b), the color of entries under V1 is darker than those under V2 (darker color indicates larger RMS error); as shown in Fig. 6, the RMS errors of inter-speed are larger than those of intra-speed in five matrices (the total mean inter-speed RMS error is $9.80°$ and the total mean intra-speed RMS error is $6.51°$). Some previous studies have started paying attention to the speed effect on joint angle estimation. Hashemi et al. [46] estimated elbow angle by sEMG signals of flexion/extension runs during constant velocity and varying velocity. Minimum %RMS errors of 8.3% and 33.3% were achieved in the two conditions, respectively. Zhang et al. [47] used EMG signals to estimate the hip, knee and ankle joint angles, and there was a $1.98°$ difference between mean RMS error of fast and slow speed under two loads. The reason of speed effect is that the higher speed increases the neuronal firing activity and therefore results in the change of muscle activity and sEMG [48]. This brings the nervous system into an unstable functional state and motion state to cause a weak estimation performance.

The sEMG signals are easily influenced by fatigue, resulting in a negative effect on estimation performance [49], [50]. In our experiment, we set a resting period between two runs to address this problem, and used subjective stop and MF test to ensure data without fatigue. It is suggested that fatigue needs to be tested and monitored in sEMG-based application although we do not focus on the fatigue effect in this study.

According to the current results, the four methods are applicable to elbow angle estimation for normal persons. However, upper-limb prostheses and exoskeletons are always used by patients after neurological injury or elderly. So the proposed methods need to be applied and verified in these people. This will be discussed in our future research.

V. Conclusion

In our study, we firstly evaluated the effect of shoulder angle variations on elbow angle estimation performance. To solve this problem, we proposed four methods: (1) using a training set including all shoulder angles' training data to train model; (2) adding two shoulder muscles' sEMG as additional inputs; (3) a two-step method using arm muscles' sEMG and two shoulder muscles' sEMG; and (4) a two-step method using arm muscles' sEMG and measured shoulder angle value by a motion sensor. The four methods reduced the mean RMS error significantly. These results show that our methods are effective to eliminate the adverse effect of shoulder angle variations and achieve a better elbow angle estimation performance. Furthermore, this study is helpful to develop a natural and stable control system for prostheses and exoskeleton systems.

Acknowledgment

This project was supported by the National Natural Science Foundation of China (No.61702454), and by the MOE (Ministry of Education in China) Project of Humanities and Social Sciences (No.17YJC870018).

References

[1] T. Lorrain, N. Jiang, and D. Farina, "Influence of the training set on the accuracy of surface emg classification in dynamic contractions for the control of multifunction prostheses," *Journal of neuroengineering and rehabilitation*, vol. 8, no. 1, p. 25, 2011.

[2] H. Su, Z. Li, G. Li, and C. Yang, “Emg-based neural network control of an upper-limb power-assist exoskeleton robot,” in *Advances in Neural Networks–ISNN 2013*. Springer, 2013, pp. 204–211.

[3] Z. Tang, S. Sun, J. Wang, and K. Zhang, “An ergonomics evaluation of the vibration backpack harness system in walking,” *International Journal of Industrial Ergonomics*, vol. 44, no. 5, pp. 753–760, 2014.

[4] F. Sylos-Labini, V. La Scaleia, A. d’Avella, I. Pisotta, F. Tamburella, G. Scivoletto, M. Molinari, S. Wang, L. Wang, E. van Asseldonk *et al.*, “Emg patterns during assisted walking in the exoskeleton,” *Frontiers in human neuroscience*, vol. 8, 2014.

[5] K. Kiguchi and Y. Hayashi, “An emg-based control for an upper-limb power-assist exoskeleton robot,” *Systems, Man, and Cybernetics, Part B: Cybernetics, IEEE Transactions on*, vol. 42, no. 4, pp. 1064–1071, 2012.

[6] M. M. White, O. N. Morejon, S. Liu, M. Y. Lau, C. S. Nam, and D. B. Kaber, “Muscle loading in exoskeletal orthotic use in an activity of daily living,” *Applied ergonomics*, vol. 58, pp. 190–197, 2017.

[7] D. Brunelli, A. M. Tadesse, B. Vodermayer, M. Nowak, and C. Castellini, “Low-cost wearable multichannel surface emg acquisition for prosthetic hand control,” in *Advances in Sensors and Interfaces (IWASI), 2015 6th IEEE International Workshop on*. IEEE, 2015, pp. 94–99.

[8] Z. Tang, K. Zhang, S. Sun, Z. Gao, L. Zhang, and Z. Yang, “An upper-limb power-assist exoskeleton using proportional myoelectric control,” *Sensors*, vol. 14, no. 4, pp. 6677–6694, 2014.

[9] D. Farina, N. Jiang, H. Rehbaum, A. Holobar, B. Graimann, H. Dietl, and O. C. Aszmann, “The extraction of neural information from the surface emg for the control of upper-limb prostheses: Emerging avenues and challenges,” *Neural Systems and Rehabilitation Engineering, IEEE Transactions on*, vol. 22, no. 4, pp. 797–809, 2014.

[10] A. Fougner, Ø. Stavdahl, P. J. Kyberd, Y. G. Losier, P. Parker *et al.*, “Control of upper limb prostheses: terminology and proportional myoelectric controlła review,” *Neural Systems and Rehabilitation Engineering, IEEE Transactions on*, vol. 20, no. 5, pp. 663–677, 2012.

[11] J. Theurel, K. Desbrosses, T. Roux, and A. Savescu, “Physiological consequences of using an upper limb exoskeleton during manual handling tasks,” *Applied ergonomics*, vol. 67, pp. 211–217, 2018.

[12] J. Ngeo, T. Tamei, T. Shibata, M. Orlando, L. Behera, A. Saxena, and A. Dutta, “Control of an optimal finger exoskeleton based on continuous joint angle estimation from emg signals,” in *Engineering in Medicine and Biology Society (EMBC), 2013 35th Annual International Conference of the IEEE*. IEEE, 2013, pp. 338–341.

[13] R. Valentini, S. Michieletto, F. Toffano, F. Spolaor, Z. Sawacha, and E. Pagello, “Emg signal analysis for online estimation of a joint angle validated through human kinematic,” *Gait & Posture*, vol. 42, pp. S13–S14, 2015.

[14] N. Araki, S. Nakatani, K. Inaya, Y. Konishi, and K. Mabuchi, “A robot prosthetic finger system based on finger joint angle estimation using emg signals,” *International Journal of Advanced Mechatronic Systems*, vol. 5, no. 6, pp. 383–390, 2013.

[15] Z. Yang, Y. Chen, J. Wang, and H. Gong, “Recognizing the breathing resistances of wearing respirators from respiratory and semg signals with artificial neural networks,” *International Journal of Industrial Ergonomics*, vol. 58, pp. 47–54, 2017.

[16] P. Erik Scheme MSc and P. Kevin Englehart PhD, “Electromyogram pattern recognition for control of powered upper-limb prostheses: State of the art and challenges for clinical use,” *Journal of rehabilitation research and development*, vol. 48, no. 6, p. 643, 2011.

[17] M. Farooq and A. A. Khan, “Effects of shoulder rotation combined with elbow flexion on discomfort and emg activity of ecrb muscle,” *International Journal of Industrial Ergonomics*, vol. 44, no. 6, pp. 882–891, 2014.

[18] E. Scheme, A. Fougner, Ø. Stavdahl, A. Chan, and K. Englehart, “Examining the adverse effects of limb position on pattern recognition based myoelectric control,” in *Engineering in Medicine and Biology Society (EMBC), 2010 Annual International Conference of the IEEE*. IEEE, 2010, pp. 6337–6340.

[19] A. Al-Timemy, R. Khushaba, G. Bugmann, and J. Escudero, "Improving the performance against force variation of emg controlled multifunctional upper-limb prostheses for transradial amputees," *Neural Systems and Rehabilitation Engineering, IEEE Transactions on*, 2015.

[20] Z. Tang, H. Yu, and S. Cang, "Impact of load variation on joint angle estimation from surface emg signals," *Neural Systems and Rehabilitation Engineering, IEEE Transactions on*, 2015.

[21] C. Cipriani, M. Controzzi, G. Kanitz, and R. Sassu, "The effects of weight and inertia of the prosthesis on the sensitivity of electromyographic pattern recognition in relax state," *JPO: Journal of Prosthetics and Orthotics*, vol. 24, no. 2, pp. 86–92, 2012.

[22] H.-J. Hwang, J. M. Hahne, and K.-R. Müller, "Channel selection for simultaneous and proportional myoelectric prosthesis control of multiple degrees-of-freedom," *Journal of neural engineering*, vol. 11, no. 5, p. 056008, 2014.

[23] A. Fougner, E. Scheme, A. C. Chan, K. Englehart, and Ø. Stavdahl, "Resolving the limb position effect in myoelectric pattern recognition," *Neural Systems and Rehabilitation Engineering, IEEE Transactions on*, vol. 19, no. 6, pp. 644–651, 2011.

[24] N. Jiang, S. Muceli, B. Graimann, and D. Farina, "Effect of arm position on the prediction of kinematics from emg in amputees," *Medical & biological engineering & computing*, vol. 51, no. 1-2, pp. 143–151, 2013.

[25] J.-J. Luh, G.-C. Chang, C.-K. Cheng, J.-S. Lai, and T.-S. Kuo, "Isokinetic elbow joint torques estimation from surface emg and joint kinematic data: using an artificial neural network model," *Journal of Electromyography and Kinesiology*, vol. 9, no. 3, pp. 173–183, 1999.

[26] R. Raj and K. Sivanandan, "Estimation of elbow joint angle from time domain features of semg signals using fuzzy logic for prosthetic control," *Int journal of current engineering and technology*, vol. 5, no. 3, pp. 2078–2081, 2015.

[27] Y. Geng, F. Zhang, L. Yang, Y. Zhang, and G. Li, "Reduction of the effect of arm position variation on real-time performance of motion classification," in *Engineering in Medicine and Biology Society (EMBC), 2012 Annual International Conference of the IEEE*. IEEE, 2012, pp. 2772–2775.

[28] K.-H. Park, H.-I. Suk, and S.-W. Lee, "Position-independent decoding of movement intention for proportional myoelectric interfaces," *Neural Systems and Rehabilitation Engineering, IEEE Transactions on*, 2015.

[29] A. Boschmann and M. Platzner, "Reducing the limb position effect in pattern recognition based myoelectric control using a high density electrode array," in *Biosignals and Biorobotics Conference (BRC), 2013 ISSNIP*. IEEE, 2013, pp. 1–5.

[30] P. Konrad, "The abc of emg," *A practical introduction to kinesiological electromyography*, vol. 1, pp. 30–35, 2005.

[31] R. Song and K. Tong, "Using recurrent artificial neural network model to estimate voluntary elbow torque in dynamic situations," *Medical and Biological Engineering and Computing*, vol. 43, no. 4, pp. 473–480, 2005.

[32] A. F. Mannion and P. Dolan, "Electromyographic median frequency changes during isometric contraction of the back extensors to fatigue." *Spine*, vol. 19, no. 11, pp. 1223–1229, 1994.

[33] S. K. Chowdhury and A. D. Nimbarte, "Effect of fatigue on the stationarity of surface electromyography signals," *International Journal of Industrial Ergonomics*, vol. 61, pp. 120–125, 2017.

[34] A. Smith and E. E. Brown, "Myoelectric control techniques for a rehabilitation robot," *Applied Bionics and Biomechanics*, vol. 8, no. 1, pp. 21–37, 2011.

[35] A.-C. Tsai, J.-J. Luh, and T.-T. Lin, "A novel stft-ranking feature of multi-channel emg for motion pattern recognition," *Expert Systems with Applications*, vol. 42, no. 7, pp. 3327–3341, 2015.

[36] N. T. Antony and P. J. Keir, "Effects of posture, movement and hand load on shoulder muscle activity," *Journal of Electromyography and Kinesiology*, vol. 20, no. 2, pp. 191–198, 2010.

[37] S. Kim, K. Nam, D. Kim, C. Ryu, Y. Kim, and J. Kim, "Optimum electrode configuration for detection of arm movement using bio-impedance," *Medical and Biological Engineering and Computing*, vol. 41, no. 2, pp. 141–145, 2003.

[38] O. Kazennikov, I. Solopova, V. Talis, A. Grishin, and M. Ioffe, "Tms-responses during anticipatory postural adjustment in bimanual unloading in humans," *Neuroscience letters*, vol. 383, no. 3, pp. 246–250, 2005.

[39] Y. Guoqing, S. Zhanyou, and A. Guochen, "Application of digitally controlled potentiometers in the intelligent sensor's measure and control system," in *Electronic Measurement and Instruments, 2007. ICEMI'07. 8th International Conference on*. IEEE, 2007, pp. 1–440.

[40] P. Mukhopadhyay, L. OSullivan, and T. J. Gallwey, "Estimating upper limb discomfort level due to intermittent isometric pronation torque with various combinations of elbow angles, forearm rotation angles, force and frequency with upper arm at 90 abduction," *International Journal of Industrial Ergonomics*, vol. 37, no. 4, pp. 313–325, 2007.

[41] B. Hudgins, P. Parker, and R. N. Scott, "A new strategy for multifunction myoelectric control," *Biomedical Engineering, IEEE Transactions on*, vol. 40, no. 1, pp. 82–94, 1993.

[42] I. Mesa, A. Rubio, I. Tubia, J. De No, and J. Diaz, "Channel and feature selection for a surface electromyographic pattern recognition task," *Expert Systems with Applications*, vol. 41, no. 11, pp. 5190–5200, 2014.

[43] H.-B. Xie, Y.-P. Zheng, J.-Y. Guo, X. Chen, and J. Shi, "Estimation of wrist angle from sonomyography using support vector machine and artificial neural network models," *Medical engineering & physics*, vol. 31, no. 3, pp. 384–391, 2009.

[44] A. D. Chan and K. B. Englehart, "Continuous myoelectric control for powered prostheses using hidden markov models," *Biomedical Engineering, IEEE Transactions on*, vol. 52, no. 1, pp. 121–124, 2005.

[45] L. Hargrove, K. Englehart, and B. Hudgins, "The effect of electrode displacements on pattern recognition based myoelectric control," in *Engineering in Medicine and Biology Society, 2006. EMBS'06. 28th Annual International Conference of the IEEE*. IEEE, 2006, pp. 2203–2206.

[46] J. Hashemi, E. Morin, P. Mousavi, and K. Hashtrudi-Zaad, "Enhanced dynamic emg-force estimation through calibration and pci modeling," *Neural Systems and Rehabilitation Engineering, IEEE Transactions on*, vol. 23, no. 1, pp. 41–50, 2015.

[47] F. Zhang, P. Li, Z.-G. Hou, Z. Lu, Y. Chen, Q. Li, and M. Tan, "semg-based continuous estimation of joint angles of human legs by using bp neural network," *Neurocomputing*, vol. 78, no. 1, pp. 139–148, 2012.

[48] N. A. Shrirao, N. P. Reddy, and D. R. Kosuri, "Neural network committees for finger joint angle estimation from surface emg signals," *Biomedical engineering online*, vol. 8, no. 1, p. 2, 2009.

[49] R. M. Enoka, S. Baudry, T. Rudroff, D. Farina, M. Klass, and J. Duchateau, "Unraveling the neurophysiology of muscle fatigue," *Journal of electromyography and kinesiology*, vol. 21, no. 2, pp. 208–219, 2011.

[50] J. Santos, J. S. Baptista, P. R. R. Monteiro, A. S. Miguel, R. Santos, and M. A. Vaz, "The influence of task design on upper limb muscles fatigue during low-load repetitive work: a systematic review," *International Journal of Industrial Ergonomics*, vol. 52, pp. 78–91, 2016.